

Adsorption character for removal Cu(II) by magnetic Cu(II) ion imprinted composite adsorbent

Yueming Ren^{a,*}, Xizhu Wei^b, Milin Zhang^a

^a Department of Material and Chemical Engineering, Harbin Engineering University, Harbin 150090, PR China

^b Department of Municipal and Environmental Engineering, Harbin Institute of Technology, Harbin 150090, PR China

Received 16 July 2007; received in revised form 12 January 2008; accepted 14 January 2008

Available online 19 January 2008

Abstract

A novel magnetic Cu(II) ion imprinted composite adsorbent (Cu(II)-MICA) was synthesized, characterized and applied for the selective removal Cu(II) from aqueous solution in the batch system. The adsorption–desorption and selectivity characteristics were investigated. The maximum adsorption occurred at pH 5–6. The equilibrium time was 6.0 h, and a pseudo-second-order model could best describe adsorption kinetics. The adsorption equilibrium data fit Langmuir isotherm equation well with a maximum adsorption capacity of 46.25 mg/g and Langmuir adsorption equilibrium constant of 0.0956 L/mg at 298 K. Thermodynamic parameters analysis predicted an exothermic nature of adsorption and a spontaneous and favourable process that could be mainly governed by physisorption mechanism. The relative selectivity coefficients of Cu(II)-MICA for Cu(II)/Zn(II) and Cu(II)/Ni(II) were 2.31, 2.66 times greater than the magnetic non-imprinted composite adsorbent (MNICA). Results suggested that Cu(II)-MICA was a material of efficient, low-cost, convenient separation under magnetic field and could be reused five times with about 14% regeneration loss.

© 2008 Elsevier B.V. All rights reserved.

Keywords: Magnetic adsorbent; Cu(II) ion imprinted; Adsorption; Heavy metals

1. Introduction

The removal of polluting heavy metals from wastewater is one of the most important issues due to their harm on human health and environment [1]. Traditional metal ion treatment processes have been studied including chemical precipitation, ion exchange, electrolysis, reverse osmosis and adsorption, etc. Each method has been found to be limited with respect to cost, complexity and efficiency. For example, the electrolysis processes often have high operational costs and the chemical precipitation may generate secondary wastes [2,3]. Among these methods, adsorption technology has been considered as an economical, efficient and promising technology in metal ion wastewater treatment [4]. Many new type or traditional adsorbents have been tested in different conditions. For example, waste fungi mycelium is attractive due to their large quantities in industry and high binding affinity to metals [5]. Chitosan (CS) is a natural

macromolecule biosorbents with many $-\text{NH}_2$ and $-\text{OH}$ groups which can serve as chelation sites to removal metals, itself is usually used in separation metal ions [6]. Using the imprinting technology, a novel Ni(II) imprinted adsorbent based on the CS and mycelium, the imprinted CS adsorbent was synthesized to improve the sole adsorption selectivity for metal ions [7–9]. However, these adsorbents suffer from a number of disadvantages such as CS is costly and the other adsorbents have low mechanical intension. Little was reported about magnetic adsorbent until now. For example, magnetic particle, magnetic-chitosan particle adsorbents with excellent and controllable properties have been reported to removal metal ions from aqueous solutions [10–13]. The main disadvantages are that the used adsorbent is possible to be easily and simply separated using the external magnetic field and will be reused.

In this study, a new method combining Cu(II) imprinting and magnetic separation technology was developed to synthesize composite adsorbent for the removal and recovery of Cu(II). The waste fungal mycelium, CS and Fe_3O_4 were employed. Considering main advantages of this adsorbent: (1) it is low

* Corresponding author. Tel.: +86 451 8256 9890; fax: +86 451 8253 3026.
E-mail address: renna815815@hotmail.com (Y. Ren).

Nomenclature

C_e	the equilibrated concentrations of metal ions (mg/L)
C_0	the initial concentrations of metal ions (mg/L)
E	removal efficiency (%)
ΔG°	the standard change in Gibbs free energy (kJ/mol)
ΔH°	the standard change in enthalpy (kJ/mol)
k_1	the first-order rate constant at the equilibrium (h^{-1})
k_2	the second-order rate constant at the equilibrium ((g/mg)/min)
K_d	the equilibrium constant (L/mg)
K_L	the affinity constant (L/mg)
q	the quality of the adsorbed metal ion for per gram adsorbent (mg/g)
q_e	the amounts of metal ions adsorbed onto adsorbent at equilibrium (mg/g)
q_m	the maximum adsorption capacity of the adsorbent (mg/g)
q_t	the amounts of metal ions adsorbed onto adsorbent at any time t (mg/g)
r^2	correlation coefficient
R	universal gas constant (8.314 J/mol K)
R_L	Langmuir dimensionless separation factor
ΔS°	the standard change in entropy (kJ/mol K)
t	time (min)
T	the temperature (K)
V	the volume of added solution (L)
W	the mass of the adsorbent (dry) (g)

cost that can be synthesized in large quantity with waste fungal mycelium from industry; (2) the adsorption selectivity is improved by imprinting technique for the target molecule (i.e. Cu(II) ions) due to molecular geometry; (3) the easy separation of magnetic composite adsorbent from treated water can be achieved by a magnetic field. Therefore, the Cu(II)-MICA was characterized by SEM, FTIR, VSM and BET. Investigations for the removal of Cu(II) ion at different pH, adsorption kinetics, isotherm, thermodynamics and selectivity were carried out to understand the mechanism of Cu(II) ion adsorption onto Cu(II)-MICA.

2. Experimental

2.1. Materials

Ammonia, ferric chloride ($\text{FeCl}_3 \cdot 6\text{H}_2\text{O}$), ferrous chloride ($\text{FeCl}_2 \cdot 4\text{H}_2\text{O}$), polystyrene, acrylamide, chitosan, epichlorhydrin, tripolyphosphate sodium, $\text{CuSO}_4 \cdot 5\text{H}_2\text{O}$, EDTA, aether, acetone and all other chemicals were reagent grade and purchased from Chemical Reagent Company of Tianjin in China. Waste fungal mycelium was provided from Harbin Pharmacy Plant in China.

2.2. Instruments

The surface morphological images of magnetic Fe_3O_4 and synthesized adsorbents were analyzed by transmission electron micrograph (TEM) (Jeol JSM-1200EXII) and scanning electron microscopy (SEM) (Quanta-200, USA), respectively.

The complexation among the synthesized adsorbents was conformed by performing FTIR (Avatar 360, NICOLET Company, USA).

Magnetic behavior was analyzed by vibrating sample magnetometer (VSM, JDM-14D, Jilin University, China).

The specific surface area and pore diameter were measured by the BET method using a Pore Size Micrometric (9320 model, USA).

The concentration of metal ion was analyzed using UV-Visible Spectrophotometer (721, Shanghai, China) in the solution.

The equipments including water boiler (DK-98-1, Tianjin, China), stirrer (JJ-8, Jiangsu, China) and vacuum oven (DZ-88, Shanghai, China) were used during the synthesis process.

An acidity meter (pHS-25, Shanghai, China) and vibrator (HY-5, Jiangsu, China) were used for pH measurement and shaking, respectively.

2.3. Synthesis of magnetic Fe_3O_4

Magnetic Fe_3O_4 was prepared by the reporting coprecipitation method [14] and our improved work. The ferrous and ferric chloride (molar ratio 1:1) were dissolved in 500 mL distilled water under nitrogen gas with vigorous stirring at 35 °C. 0.5 M ammonia aqueous of about 30 mL (29%) was added quickly into the solution. The color of bulk solution turned from orange to black immediately. Then it was kept with the hydrothermal treatment at 80 °C for 1.5 h and separated under a magnetic field. The magnetite was decorated with polystyrene and acrylamide by ultrasonic treatment for 30–60 min. Then the solution was raised to 60–80 °C and cooled down after being stirred at 700 rpm for 4.0 h. The magnetic particle was separated again and dried in a vacuum oven at 60 °C after being washed several times with water and ethanol.

2.4. Synthesis of adsorbents

Cu(II)-MICA was prepared as shown in Fig. 1. 0.2 g CS was dissolved in 10 mL dilute acetic acid solution of 2.5% (v/v) with mechanical stirring. 5 mL CuSO_4 solution of 5000 mg/L was added. After stirring for 6.0 h at 25 °C, the mixture was washed by distilled water, ethanol and aether time after time. Afterward, 0.5 g Fe_3O_4 and 0.3 mL epichlorhydrin (crosslinking reagent) were added with vigorous stirring for 3.0 h at 30 °C to complete the crosslinking reaction. Then 0.2 g waste fungal mycelium (dry weight), 10 mL tripolyphosphate sodium solution (counteracting acetic acid and fixing the outer film of the synthesized composite adsorbent) of 2.5% (g/L) and 20 mL-distilled water were added, and then the mixture was fixed for 8.0 h at 25 °C after stirring for 15 min. Then the Cu(II) imprinted in the adsorbent was removed by 0.2 M EDTA for 2.0 h at 25 °C. Regeneration was carried

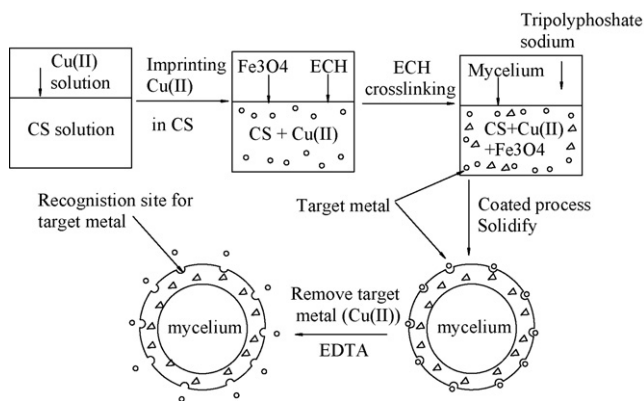


Fig. 1. Preparation schematic illustration of Cu(II)-MICA.

out by washing the adsorbent with 0.2 M NaOH for 1.0 h by resuspension at shaking bath. The synthesized adsorbent was washed several times with distilled water and acetone, followed by filtration and dryness at 60 °C. The dry adsorbent was whetted to obtain narrow size distributions and stored at a sealed bottle for further use. The MNICA was prepared in a similar way without Cu(II) imprinting and removal process.

2.5. Cu(II) adsorption–desorption experiments

Adsorption of Cu(II) from aqueous solutions was investigated in batch experiments. Effects of pH (2–6), kinetic experiments (0–12 h), adsorption isotherm (20–300 mg/L initial Cu(II) concentration) and thermodynamic studies (298–328 K) on adsorption were studied. The experiment conditions were modulated according to the requirement. All the adsorption experiments were carried out at 25 °C, in which pH was maintained in a range of 5.5 ± 0.1 units, adsorbent concentration was kept constant at 10 mg in 20 mL solution, initial Cu(II) concentration was 100 mg/L, equilibrium time was kept as 6.0 h, except stated otherwise.

After adsorption reached equilibrium, the adsorbent was separated via an external magnetic field (except non-magnetic adsorbent). The concentration of Cu(II) ion in the solution was analyzed by following the standard methods [15]. For each set of data presented, standard statistical methods were used to determine the mean values and standard deviations. Confidence intervals of 95% were calculated for each set of samples in order to determine the margin error. Adsorption values were calculated from the change in solution concentration using the following equation [16]:

$$q = \frac{(C_0 - C_e)V}{W} \quad (1)$$

where q (mg/g) adsorption capacity; C_0 (mg/L) and C_e (mg/L) initial and equilibrated metal ion concentrations, respectively, V (L) volume of added solution and W (g) the mass of the adsorbent (dry).

$$E = \frac{C_0 - C_e}{C_0} \times 100\% \quad (2)$$

where E (%) removal efficiency.

Desorption of Cu(II) ions was studied in 20 mL 0.2 M EDTA solution. 0.1 g Cu(II)-MICA was dipped in this desorption medium and stirred continuously at a 700 rpm for 60 min at 25 °C. Metal ion concentrations in the solution were analyzed at different desorption time and the desorption ratio ($D\%$) was calculated as Eq. (3) [17]:

$$D\% = \frac{\text{metal ion desorbed to the EDTA solution (mg/L)}}{\text{metal ion adsorbed onto adsorbent (mg/L)}} \quad (3)$$

In order to test the reusability of Cu(II)-MICA, Cu(II) sorption–desorption procedure was repeated five times. After each cycle, the Cu(II)-MICA was washed thoroughly with deionised water to neutrality and dried in a vacuum oven at 50 °C for adsorption in the succeeding cycle.

2.6. Selectivity experiments

In order to prove Cu(II) specificity of Cu(II)-MICA, Zn(II) and Ni(II) were chosen as competitive metal ions. Each concentration of Cu(II), Zn(II) and Ni(II) was 50 mg/L in the mixed solution. Cu(II)-MICA and MNICA were treated with these competitive ions. After adsorption equilibrium, the concentration of each ion in the remaining solution was measured. Distribution and selectivity coefficients of Zn(II) and Ni(II) with respect to Cu(II) were calculated as the followings [18]:

$$K_d = \left(\frac{C_0 - C_e}{C_e} \right) \frac{V}{W} \quad (4)$$

where K_d the distribution coefficient (mL/g).

$$K = \frac{K_d(\text{Cu(II)})}{K_d(\text{M(II)})} \quad (5)$$

where K is the selectivity coefficient and M(II) represents Zn(II) or Ni(II) ions. A comparison of the K values of Cu(II)-MICA with those metal ions allows an estimation of the effect of imprinting on selectivity. A relative selectivity coefficient (K') is an indicator to express metal adsorption affinity of recognition sites to the imprinted Cu(II) ions, which can be defined by Eq. (6):

$$K' = \frac{K_{\text{imprinted}}}{K_{\text{non-imprinted}}} \quad (6)$$

3. Result and discussion

3.1. Characterization of adsorbent

Fig. 2 illustrated the TEM photograph of magnetite. It revealed that the maghemite nanoparticles synthesized in this study were multidispersed well with a particle size of about 10 nm. SEM images (Fig. 3a and b) showed that Cu(II)-MICA was irregular clump and had a rough surface with an average diameter of around 200 μm . The BET surface area was 52.32 m^2/g and average pore diameter was 16.7 nm. However, no significantly different morphology is observed for MNICA (the images are not listed here). The BET surface area was 39.95 m^2/g and average pore diameter is 4.9 nm.

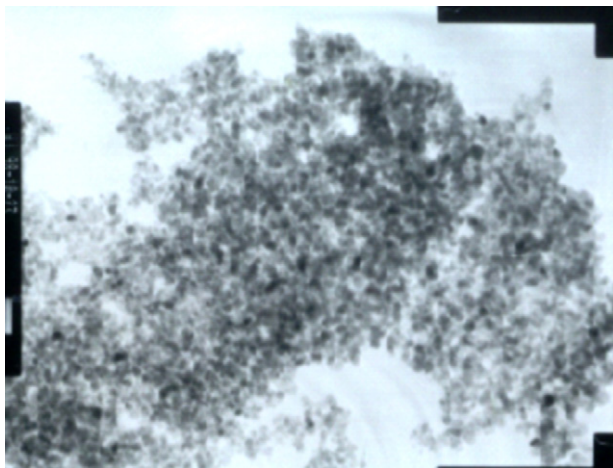


Fig. 2. TEM of magnetic Fe_3O_4 stabilized distribution.

The FTIR spectra of CS, Fe_3O_4 and prepared adsorbents were shown in Fig. 4. Fig. 4b showed the basic characteristic peaks of CS at: $3260\text{--}3410\text{ cm}^{-1}$ (O–H and N–H stretching), 2925 and 2854 cm^{-1} (C–H stretching combining with hydroxyls on methyl and methylene), 1641 cm^{-1} (C=O of –NH–C=O stretching), 1519 cm^{-1} (N–H bending), 1086 and 1026 cm^{-1} (C–OH stretching). In Fig. 4a, the peaks at 597 cm^{-1} attributed to the Fe–O bond vibration. The synthesized Fe_3O_4 were decorated with abundant amido and hydroxy groups. Comparing Fig. 4c and d, the characteristic peaks at $3260\text{--}3410$, 1641 and 1519 cm^{-1} became weak. This could be attributed to the depletion of hydroxyls or amidos groups in the binding reaction. The peaks at 1026 disappeared and at 1086 cm^{-1} became strong, which explained the crosslinking had reacted with hydroxyls and became C–O–C. The peaks at 2925 and 2854 cm^{-1} became weak with illustration of reduction of hydroxyls.

The magnetic property was studied. As shown in Fig. 5, the greatest saturation magnetization (M_s) and remanent magnetization (M_r) of Cu(II)-MICA were 4.2 and 0.9 emu/g , respectively. Compared with the M_s and M_r value (46.5 and 11.9 emu/g) for the naked Fe_3O_4 nanoparticles, there was a slightly lower value for the magnetic adsorbent. However, Cu(II)-MICA exhibits similar superparamagnetic properties like Fe_3O_4 and has a good

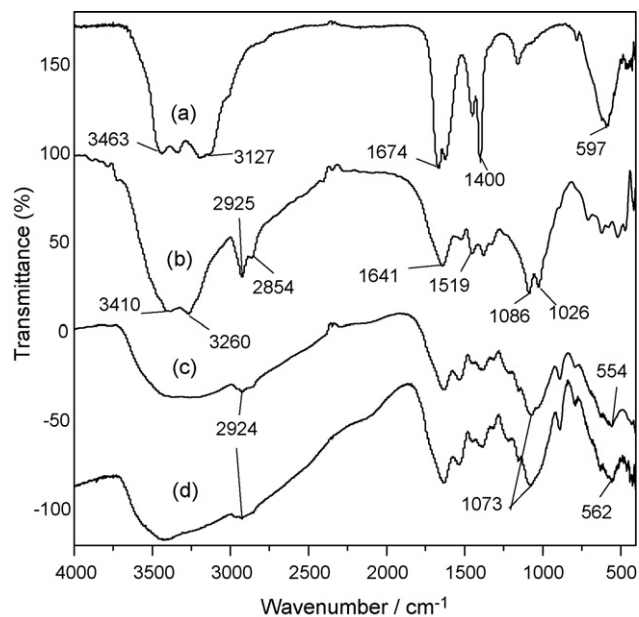


Fig. 4. FTIR spectrum of (a) Fe_3O_4 , (b) CS, (c) Cu(II)-MICA and (d) MNICA.

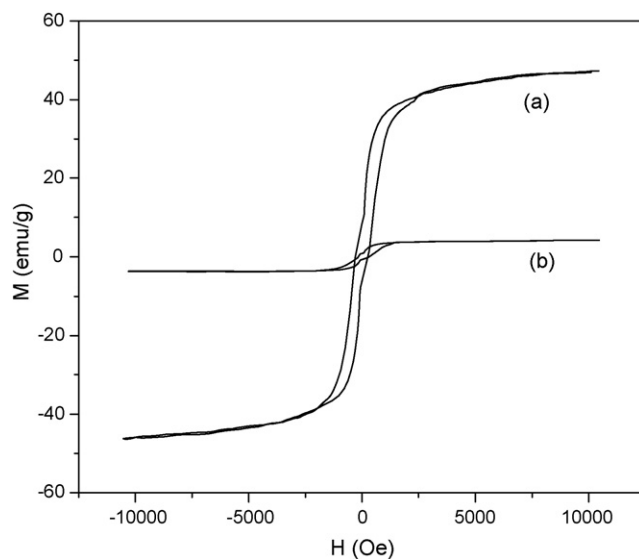


Fig. 5. The magnetic hysteresis loop of (a) Fe_3O_4 and (b) Cu(II)-MICA.

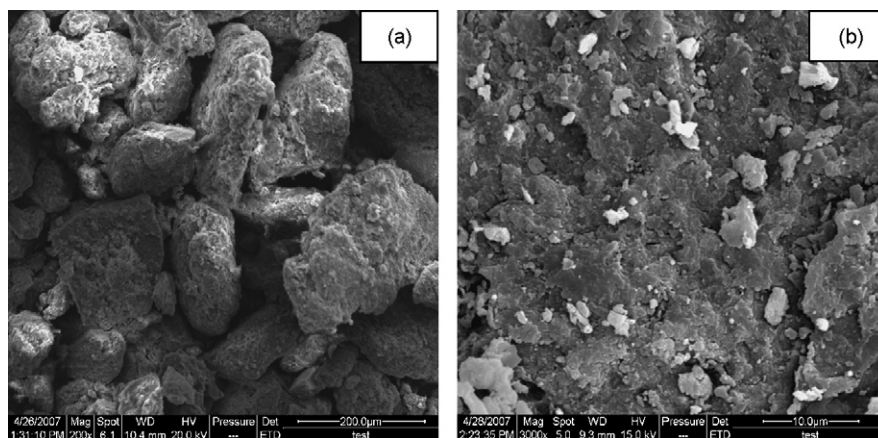


Fig. 3. SEM micrographs of Cu(II)-MICA with different magnification: (a) $200\times$ and (b) $3000\times$.

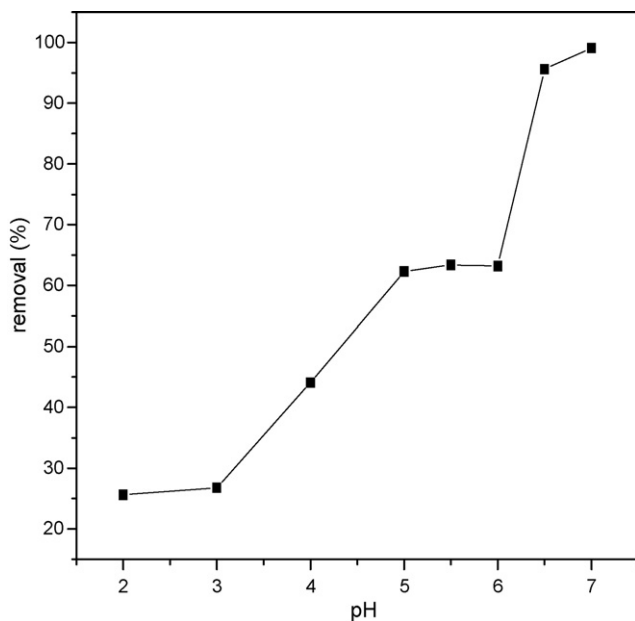


Fig. 6. Effect of pH on adsorption capacity of Cu(II) onto Cu(II)-MICA.

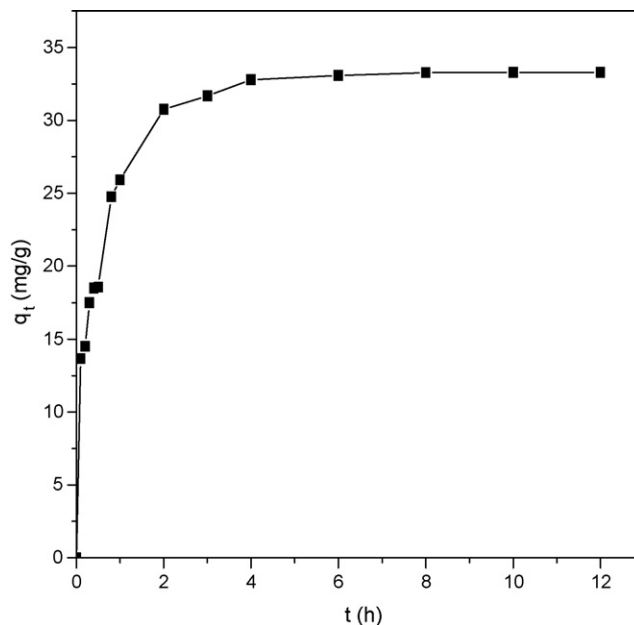


Fig. 7. Adsorption kinetics of Cu(II)-MICA for Cu(II) ion.

response under the additional permanent magnetization, which made the solid and liquid phases separate quickly.

3.2. Effect of pH

The pH is one of the most important parameters governing the uptake of metal ions on adsorbents [19]. The effect of various pH on Cu(II) ion removal by Cu(II)-MICA was shown in Fig. 6. At pH 2–3 the sorption was low, possibly because of an excess of hydrogen ions can compete effectively with Cu(II) for bonding sites. This condition may be utilized for desorption of Cu(II) ion from the adsorbent. At higher pH values of 3–5, adsorption functional groups such as carboxyl or hydroxyl were deprotonated and negatively charged. Consequently, the attraction of positively charged Cu(II) ion enhanced. At pH values of 5–6 the increasing rate was relatively very slow. After pH 6.5, the reason for the sharp increase removal was that the Cu(II) began to precipitate as Cu(OH)₂. So Cu(II) ion were removed by both adsorption and precipitation above precipitation pH 6.5. As a result, the optimum pH for Cu(II) ion sorption was found in the pH range 5–6, and all further experiments were carried out at pH 5.5.

3.3. Adsorption kinetics

The effect of contact time on the Cu(II)-MICA adsorption from solution was given in Fig. 7. The adsorption occurred rapidly at the early stage of the reaction, which was probably due to the abundant availability of active sites on the adsorbents, and with the gradual decrease of active sites slowing down the ions exchange action from bulk solution. From 2.0 to 6.0 h of reaction, the adsorption amount increased very slowly which indicated equilibrium condition. As a result, the adsorption time of 6.0 h was optimal.

The prediction of adsorption rate gives important information for selecting optimum operating conditions for full-scale batch process. In order to investigate the mechanism of adsorption kinetics, two different kinetic models were tested to interpret data obtained from batch experiments. The pseudo-first-order rate equation of Lagergren and Kungliga [20] is given as:

$$\log(q_e - q_t) = \frac{\log q_e - k_1 t}{2.303} \quad (7)$$

where q_e and q_t the amounts of Cu(II) adsorbed onto adsorbent at equilibrium and any time t (mg/g), respectively, k_1 the first-order rate constant at the equilibrium (h^{-1}). When the experimental data was plotted in form of $\log(q_e - q_t)$ versus t , a straight line would be obtained if the pseudo-first-order kinetic model was a suitable expression. The rate constant (k_1) can be obtained from the slope of the line.

Assuming that the adsorption capacity of adsorbent is proportional to the number of active sites on its surface, the pseudo-second-order rate equation developed by Ho and McKay [20] is as the following:

$$\frac{t}{q_t} = \frac{1}{k_2 q_e^2} + \frac{1}{q_e} t \quad (8)$$

where k_2 the second-order rate constant at the equilibrium ($(\text{g}/\text{mg})/\text{min}$). Thus, by plotting t/q_t against t , the values of k_2 ($\text{slope}^2/\text{intercept}$), q_e ($1/\text{slope}$) can be determined graphically from the slope and intercept of the revealed plots.

As seen from Fig. 8a and b, the correlation coefficients (r^2) given by the two kinetic models were 0.9948 and 0.9996, respectively. Obviously, the pseudo-second-order kinetic model gave a good correlation for the adsorption of Cu(II) ions on Cu(II)-MICA. The adsorption kinetic constants and linear regression values with standard deviation were summarized in Table 1. The theoretical q value estimated from pseudo-second-order kinetic model was very close to the experimental

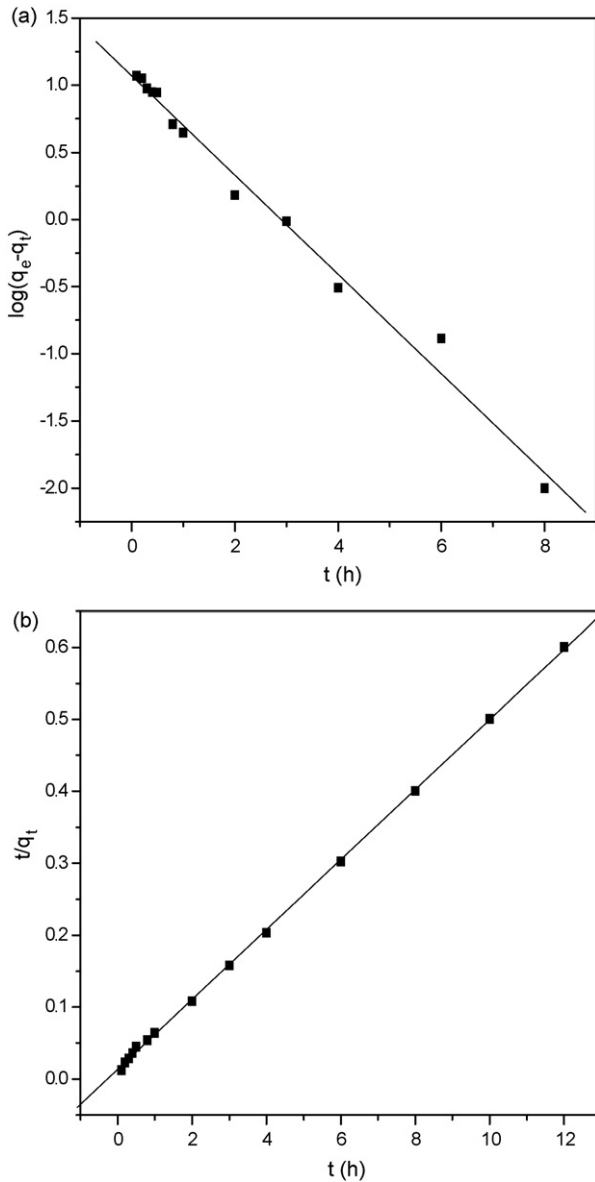


Fig. 8. The linear plot of (a) $\log(q_e - q_t)$ vs. t and (b) t/q_e vs. t .

value. These values showed that this adsorbent system was not described by pseudo-first-order kinetic model. So, the results suggested that the pseudo-second-order adsorption mechanism was predominant for this adsorbent system and that the overall rate of the Cu(II) adsorption process appeared to be controlled by chemical reaction. The rate constant k_2 determined was 0.1923 (g/mg)/min. The max capacity was less than the value from Langmuir isotherm equation, which might be because Cu(II) ion initial concentration was lower

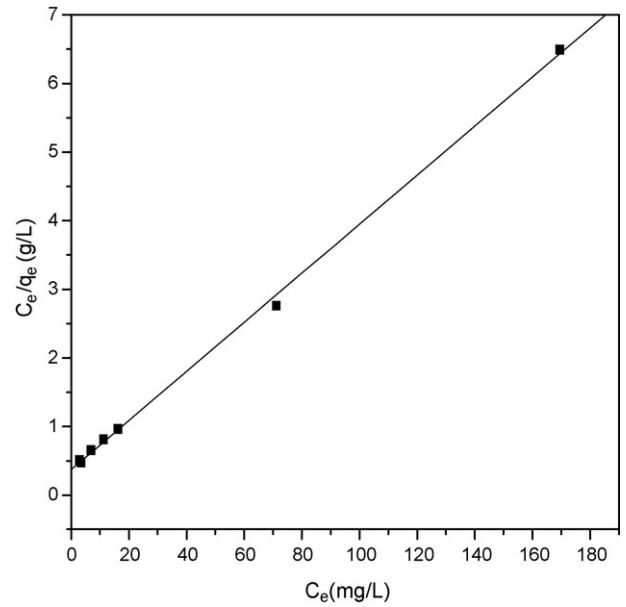


Fig. 9. Linear isotherm plots of Langmuir isotherm for Cu(II)-MICA.

than that of achieving equilibrium in adsorption isotherm experiment.

3.4. Adsorption isotherm

Adsorption isotherm of Cu(II) onto the prepared Cu(II)-MICA was similar to the Langmuir sorption isotherm at 25 °C. An adsorption isotherm provides a relationship between the ion concentration in the solution and the amount of ion adsorbed on the solid phase when the two phases are at equilibrium. The Langmuir sorption isotherm assumes monolayer coverage of the adsorption surface, the adsorption sites are also assumed to be energetically equivalent and distant to each other so that there are no interactions between molecules adsorbed to adjacent sites [21]. It is expressed as:

$$q_e = \frac{q_m K_L C_e}{1 + K_L C_e} \quad (9)$$

where q_e the amount of Cu(II) adsorbed per unit weight of adsorbent at equilibrium (mg/g), C_e the equilibrium concentration of Cu(II) ions in solution (mg/L), q_m the maximum adsorption capacity of the adsorbent (mg/g), K_L the affinity constant (L/mg). The values of q_m and K_L can calculate from the intercept and slope of the linear plot of C_e/q_e against C_e .

Fig. 9 showed the fitted equilibrium data in Langmuir isotherm expressions for Cu(II)-MICA. The correlation coefficient (r^2) was 0.9996. The Langmuir adsorption model can be applied in this affinity adsorbent system. From the slope and

Table 1
Kinetic parameters of the pseudo-order rate equation for Cu(II) adsorption onto Cu(II)-MICA

Experimental q (mg/g)	Pseudo-first-order rate equation				Pseudo-second-order rate equation			
	k_1 (h^{-1})	q (mg/g)	r_1^2	S.D.	k_2 ((g/mg)/min)	q (mg/g)	r_2^2	S.D.
29.85	0.8438	23.63	0.9948	0.09039	0.1923	30.53	0.9996	0.00403

Table 2
 R_L values in Langmuir isotherm of Cu(II)-MICA

C_0 (mg/L)	R_L
20	0.343407
40	0.207297
60	0.148456
80	0.115634
100	0.094697
200	0.049702
300	0.033693

intercept, the values of q_m and K_L were found to be 46.25 mg/g and 0.0956 L/mg.

It also assumes that all the binding sites on the sorbent are free sites, ready to accept the sorbent from solution. The affinity between Cu(II) ion and Cu(II)-MICA can be predicted using Langmuir dimensionless separation factor R_L given by relation [22]:

$$R_L = \frac{1}{1 + K_L C_0} \quad (10)$$

where C_0 the initial Cu(II) concentration (mg/L). Others researcher [22] had shown R_L indicated the shape of the isotherm, value of $R_L < 1$ represented the favourable adsorption and value $R_L > 1$ represented unfavourable adsorption. The values of R_L were shown in Table 2. In our study R_L were all found to be within 0 and 1 that indicated a highly favourable adsorption with increasing adsorption efficiency at higher Cu(II) concentrations.

3.5. Adsorption thermodynamics

The effect of temperature on the adsorption equilibrium of Cu(II) ion onto Cu(II)-MICA was investigated. Adsorption of Cu(II) increased as the temperature increased from 298 to 328 K (figure is not listed here). Based on fundamental thermodynamics concept, supposing that the reaction is in an isolated system, system energy cannot be gained or lost and the entropy change is the only driving force. In order to gain insight into the mechanism involved in the adsorption, the variations including standard Gibbs free energy (ΔG°), enthalpy (ΔH°) and entropy change (ΔS°) for the adsorption were calculated from the slope and intercept from the plots of $\log K_d$ versus $1/T$ (Fig. 10) according to Eqs. (11)–(13) [23]. The values of thermodynamic parameters calculated are shown in Table 3.

$$K_d = \frac{q_e}{C_e} \quad (11)$$

$$\log K_d = \frac{\Delta S^\circ}{R} - \frac{\Delta H^\circ}{RT} \quad (12)$$

Table 3
 Thermodynamic parameters for Cu(II) adsorption onto Cu(II)-MICA

C_0 (mg/L)	ΔH° (kJ/mol)	ΔS° (kJ/mol K)	ΔG° (kJ/mol)			
			298 K	308 K	318 K	328 K
100	10.70	0.04	−1.22	−1.62	−2.02	−2.42

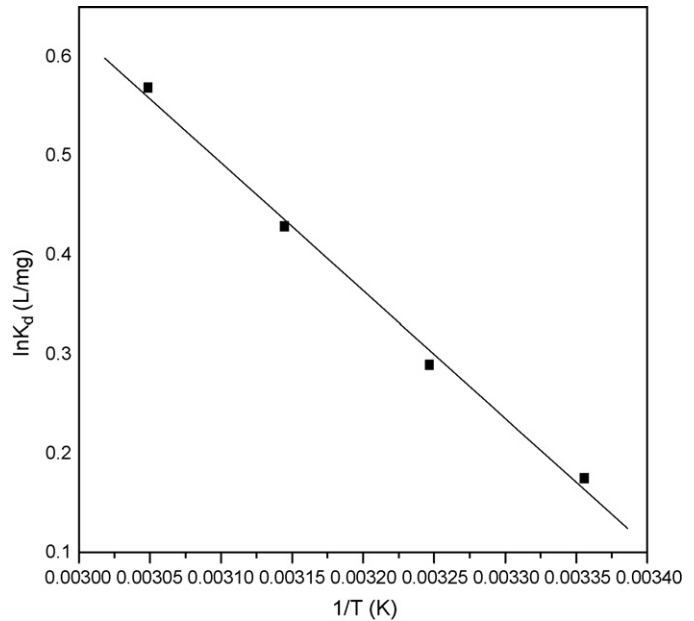


Fig. 10. The plots of $\log K_d$ vs. $1/T$ for Cu(II)-MICA.

$$\Delta G^\circ = \Delta H^\circ - T\Delta S^\circ \quad (13)$$

where K_d the same meaning in Eq. (4), q_e and C_e meaning representing in Eq. (6). ΔS° the standard change in entropy (kJ/mol K), ΔH° the standard change in enthalpy (kJ/mol), ΔG° the standard change in Gibbs free energy (kJ/mol), T the temperature (K) and R universal gas constant (8.314 J/mol K).

Positive ΔH° (10.7 kJ/mol) value indicated the endothermic nature of adsorbent, which fact was supported by the increase in the adsorption of Cu(II) with temperature. Literature [24] suggested that ΔH° of physisorption is smaller than 40 kJ/mol. This study suggested ion-exchange may play a significant role in the adsorption process. Furthermore, ΔG° (from −1.22 to −2.42 kJ/mol) was negative verifying that Cu(II) adsorption was spontaneous and thermodynamically favourable. ΔG° decreased further with increase in temperature implies a greater driving force and more spontaneous adsorption at high temperature. The positive ΔS° (0.04 kJ/mol K) revealed that the degrees of freedom increased at the solid–liquid interface during the adsorption and it might be related to the substitution of water hydration molecules of metal ion by different chelating groups.

3.6. Adsorption selectivity

Zn(II) and Ni(II) were chosen as competitive metal ions because of their similar ionic radii (Cu(II): 73 pm, Zn(II): 74 pm, Ni(II): 69 pm). Our experiment had confirmed the capacity could achieve a maximum at pH 5.5 in their pure aqueous solution.

Table 4
 K_d , K and K' values of Zn(II) and Ni(II) with respect to Cu(II)

Metal ions	MNICA		Cu(II)-MICA		K'
	K_d (mL/g)	K	K_d (mL/g)	K	
Cu(II)	124	–	210	–	–
Zn(II)	116	1.07	85	2.47	2.31
Ni(II)	58	2.13	37	5.67	2.66

Table 4 summarizes K_d , K and K' values of Zn(II) and Ni(II) with respect to Cu(II). When they existed in the same medium, a competition would start for the same attachment sites. The Cu(II) sorption capacity of the Cu(II)-MICA was much higher than that for other metal ions. A comparison of the K_d values for the Cu(II) imprinted adsorbent with the control samples showed an increase in K_d for Cu(II) while K_d decrease for Zn(II) and Ni(II). The relative selectivity coefficient is an indicator to express an adsorption affinity of recognition sites to the imprinted Cu(II) ions. The results showed that relative selectivity coefficients of Cu(II)-MICA for Cu(II)/Zn(II) and Cu(II)/Ni(II) were 2.31, 2.66 times greater than MNICA, respectively (Table 4). It should be noted that the imprinted beads showed selectivity for the target molecule (i.e. Cu(II) ions) due to molecular geometry. This means that Cu(II) ions can be determined even in the presence of Zn(II) and Ni(II) interferences.

3.7. Desorption and repeated use

The regeneration of the adsorbent is likely to be a key factor in improving wastewater process economics. Desorption of Cu(II) ions from the Cu(II)-MICA was performed in a batch experimental set-up. In this study, the desorption time was found to be 20 min. Desorption ratios could be up to 92%. In order to obtain the reusability of the Cu(II)-MICA, adsorption–desorption cycles were repeated five times by using the same magnetic imprinted adsorbent. The adsorption capacity of the recycled Cu(II)-MICA was about 14% loss at the 5th cycle. It can be concluded that the Cu(II)-MICA can be used many times without decreasing their adsorption capacities significantly.

4. Conclusions

A novel Cu(II)-MICA was prepared and characterized using the SEM, FTIR, VSM and surface area, pore diameter by BET studies. Characteristics of pH effect, equilibrium, kinetics, thermodynamics, selectivity sorption and desorption which are used as adsorbents for Cu(II) were tested. The results showed that it was amorphous and the complexation in Cu(II)-MICA was through amide and hydroxy groups, etc. It exhibited superparamagnetic properties with a saturation magnetization of 4.2 emu/g and a remanent magnetization of 0.9 emu/g, respectively. The surface area and pore diameter of Cu(II)-MICA improved greatly. In addition, the Cu(II)-MICA was quite efficient for the removal of Cu(II) ions from aqueous solutions at pH 5–6. The adsorption equilibrium time was 6.0 h, and Cu(II)

adsorption process onto Cu(II)-MICA could be best described by the pseudo-second-order model. The adsorption behavior followed the Langmuir adsorption isotherm with a maximum adsorption capacity of 46.25 mg/g and a Langmuir adsorption equilibrium constant of 0.0956 L/mg at 25 °C. Langmuir dimensionless separation factor calculation results indicated that a highly favourable adsorption with increased adsorption efficiency was at higher Cu(II) ion concentrations. Thermodynamic parameters suggested that the adsorption process was spontaneous and governed by physisorption interaction, the adsorption was a spontaneous process at high temperature and endothermic in nature. The relative selectivity coefficient is an indicator to express an adsorption affinity of recognition sites to the imprinted Cu(II). The results showed that K_d of Cu(II)-MICA for Cu(II)/Zn(II) and Cu(II)/Ni(II) were 2.31, 2.66 times greater than MNICA, respectively. The desorption time was found to be 20 min. The Cu(II)-MICA can be used five times without decreasing their adsorption capacities significantly.

References

- [1] Y. Nuhoglu, E. Oguz, Removal of copper(II) from aqueous solutions by biosorption on the cone biomass of *Thuja orientalis*, Proc. Biochem. 38 (2003) 1627–1631.
- [2] J.G. Dean, F.L. Bosqui, K.L. Lannouette, Removing heavy metals from wastewater, Environ. Sci. Technol. 6 (1997) 518–524.
- [3] G. Donmez, Z. Aksu, The effect of copper(II) ions on the growth and bioaccumulation properties of some yeast, Proc. Biochem. 35 (1999) 135–142.
- [4] F. Ekmekyapar, A. Aslan, Y. Kemal Bayhan, A. Cakici, Biosorption of copper(II) by nonliving lichen biomass of *Cladonia rangiformis* hoffm., J. Hazard. Mater. B 137 (2006) 293–298.
- [5] A. Kapoor, T. Viraraghavan, D.R. Cullimore, Removal of heavy metals using the fungus *Aspergillus niger*, Biores. Technol. 70 (1999) 95–104.
- [6] K.Z. Knaul, S.M. Hucson, K.A.M. Creder, Improved mechanical properties of chitosan fibers, J. Appl. Polym. Sci. 72 (1999) 1721–1732.
- [7] T.W. Tan, X.J. He, W.X. Du, Adsorption behaviour of metal ions on imprinted chitosan adsorbent, J. Chem. Technol. Biotechnol. 76 (2001) 191–195.
- [8] H.J. Su, Z.X. Wang, T.W. Tan, Preparation of a surface molecular-imprinted adsorbent for Ni²⁺ based on *Penicillium chrysogenum*, J. Chem. Technol. Biotechnol. 80 (2005) 439–444.
- [9] H.J. Su, Y. Zhao, J. Li, T.W. Tan, Biosorption of Ni²⁺ by the surface molecular imprinting adsorbent, Proc. Biochem. 41 (2006) 1422–1426.
- [10] J. Hu, M.C. Lo, G.H. Chen, Adsorption of Cr(VI) by magnetite nanoparticles, Water Sci. Technol. 50 (2004) 139–146.
- [11] Y.-C. Chang, D.-H. Chen, Preparation and adsorption properties of monodisperse chitosan-bound Fe₃O₄ magnetic nanoparticles for removal of Cu(II) ions, J. Colloid Interface Sci. 283 (2005) 446–451.
- [12] J. Hu, G. Chen, I.M.C. Lo, Removal and recovery of Cr(VI) from wastewater by maghemite nanoparticles, Water Res. 39 (2005) 4528–4536.
- [13] Y.-C. Chang, S.-W. Chang, D.-H. Chen, Magnetic chitosan nanoparticles: studies on chitosan binding and adsorption of Co(II) ions, React. Funct. Polym. 66 (2006) 335–341.
- [14] C. Qus, H.B. Yang, D.W. Ren, Magnetite nanoparticles prepared by precipitation from partially reduced ferric chloride aqueous solutions, J. Colloid Interface Sci. 215 (1999) 190–192.
- [15] APHA, AWWA, Standard Methods for Examination of Water and Wastewater, 20th ed., APHA, AWWA, Washington, DC, New York, 1998.
- [16] Y. Prasanna Kumar, P. King, V.S.R.K. Prasad, Adsorption of zinc from aqueous solution using marine green algae—*Ulva fasciata* sp., Chem. Eng. J. 129 (2007) 161–166.
- [17] E. Pehlivan, S. Cetin, B.H. Yanyk, Equilibrium studies for the sorption of zinc and copper from aqueous solutions using sugar beet pulp and fly ash, J. Hazard. Mater. B 135 (2006) 193–199.

- [18] H. Yavuz, R. Sayb, A. Denizli, Iron removal from human plasma based on molecular recognition using imprinted beads, *Mater. Sci. Eng. C* 25 (2005) 521–528.
- [19] V.C. Taty-Costodes, H. Fauduet, C. Porte, A. Delacroix, Removal of Cd(II) and Pb(II) ions from aqueous solutions by adsorption onto sawdust of *Pinus sylvestris*, *J. Hazard. Mater. B* 105 (2003) 121–142.
- [20] Y.S. Ho, G. McKay, Kinetic models for the sorption of dye from aqueous solution by wood, *Trans. Inst. Chem. Eng.* 76B (1998) 183–191.
- [21] Y.S. Ho, G. McKay, Batch lead (II) removal from aqueous solution by peat: equilibrium and kinetics, *Trans. Inst. Chem. Eng.* 77B (1999) 165–173.
- [22] Benhammou, A. Yaacoubi, L. Nibou, B. Tanouti, Adsorption of metal ions onto Moroccan stevensite: kinetic and isotherm studies, *J. Colloid Interface Sci.* 282 (2005) 320–324.
- [23] Z. Reddad, C. Gerente, Y. Andres, P. Le Cloirec, Adsorption of several metal ions onto a low-cost biosorbent: kinetic and equilibrium studies, *Environ. Sci. Technol.* 36 (2002) 2067–2073.
- [24] S. Ricordel, S. Taha, I. Cisse, G. Dorange, Heavy metals removal by adsorption onto peanut husks carbon: characterization, kinetic study and modeling, *Sep. Purif. Technol.* 24 (2001) 389–401.